

In Silico Studies of Indole Derivatives as Antibacterial Agents

Mridul Shah^{1†}, Adarsh Kumar^{1†}, Ankit Kumar Singh¹, Harshwardhan Singh¹, Balasubramanian Narasimhan², Pradeep Kumar^{1*}

¹Department of Pharmaceutical Sciences and Natural Products, Central University of Punjab, Ghudda, Bathinda, India

²Department of Pharmaceutical Sciences, Maharshi Dayanand University, Rohtak, Haryana, India

Received June 5, 2022

Reviewed July 2, 2022

Accepted December 12, 2022

*Corresponding Author

Pradeep Kumar
Department of Pharmaceutical
Sciences and Natural Products, Central
University of Punjab, Ghudda, Bathinda,
BP151401, India
Tel: +98-10-1377-4553
E-mail: pradeepyadav27@gmail.com

[†]These authors contributed equally to this work.

Objectives: Molecular docking and QSAR studies of indole derivatives as antibacterial agents.

Methods: In this study, we used a multiple linear regressions (MLR) approach to construct a 2D quantitative structure activity relationship of 14 reported indole derivatives. It was performed on the reported antibacterial activity data of 14 compounds based on theoretical chemical descriptors to construct statistical models that link structural properties of indole derivatives to antibacterial activity. We have also performed molecular docking studies of same compounds by using Maestro module of Schrodinger. A set the molecular descriptors like hydrophobic, geometric, electronic and topological characters were calculated to represent the structural features of compounds. The conventional antibiotics sultamicillin and ampicillin were not used in the model development since their structures are different from those of the created compounds. Biological activity data was first translated into pMIC values (i.e. $-\log \text{MIC}$) and used as a dependent variable in QSAR investigation.

Results: Compounds with high electronic energy and dipole moment were effective antibacterial agents against *S. aureus*, indole derivatives with lower κ_2 values were excellent antibacterial agents against MRSA standard strain, and compounds with lower R value and a high $^2\chi^v$ value were effective antibacterial agents against MRSA isolate.

Conclusion: Compounds 12 and 2 showed better binding score against penicillin binding protein 2 and penicillin binding protein 2a respectively.

Keywords: 2D QSAR, antibacterial, MLR, indole, pMIC, molecular docking

INTRODUCTION

In the 1670s, Van Leeuwenhoek first identified bacteria, a single-cell organism. Later, in the 19th century, several concepts highlighting the strong correlation between bacteria and diseases were developed. This encouraged many researchers to develop antibacterial agents. In 1928, Sir Alexander Fleming discovered penicillin from *Penicillium notatum*, and this discovery unlocked the development of many agents that were able to either kill bacteria or inhibit bacterial growth [1]. The discovery of antibacterial agents helped to increase the human life span, but irrational use of these agents led to the rise of bacterial resistance.

Resistance is associated with excessive use or misuse of antibacterial drugs in humans, animal farming, and agriculture [2], and is an increasingly severe worldwide problem. Various new antibacterial drugs have been developed, but bacteria have become resistant to most of these [3]. The number of infections by pathogenic microorganisms that are resistant to the newer or current antibiotics is rising, and invasive bacterial infections are now more common than at the beginning of the century. Infectious diseases are the world's major risk to human health and life [4].

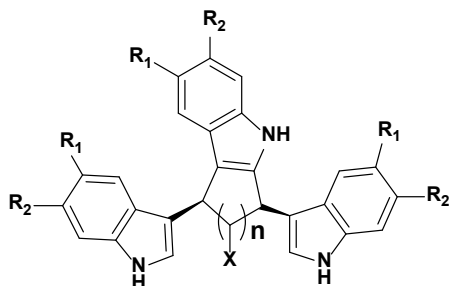
The indole moiety is a medically relevant scaffold that is widely identified as a pharmacophore structure. An indole nucleus is present in compounds involved in research aimed

at evaluating new products that possess beneficial biological properties such as anti-fungal [5], anti-tubercular [6], anti-inflammatory [7], antipsychotic [8], anticancer [9], antimicrobial [10], antioxidant [11], anticonvulsant [12], antileishmanial [13], anthelmintic [14], antiviral, antimicrobial, antidiabetic, and antidepressant [15] activities. The indole ring system became an essential part of the structure of many pharmacological medicines, which is not surprising. Substituted indole is a favored structure because of its ability to bind to a wide range of targets with high affinity. The indole frame is one of the most beautiful frameworks, with a wide range of biological and pharmacological activities. This physiologically important nucleus is present in a large number of therapeutic agents and natural products. The occurrence and availability of indole compounds are widespread in nature, and a large number of them exhibit biological activity. Substitution of the indole ring by other heterocycles is often accompanied by the loss of biological activity. The indole ring system is found in a wide variety of naturally occurring compounds, which include tryptophan, an essential amino acid, 3-indoleacetic acid, the main growth hormone in higher plants, and serotonin, an important neurotransmitter in animals that plays a key role in our mental health [16-18].

1. Quantitative structure-activity relationship

Quantitative structure-activity relationship (QSAR) and quantitative structure-property relationship models are used

Table 1. Chemical structure of substituted indole derivatives



Compound no.	N	X	R ₁	R ₂
1	1	H	H	H
2	1	Cl	H	H
3	1	Br	H	H
4	2	H	H	H
5	2	H	Cl	H
6	2	H	H	Cl

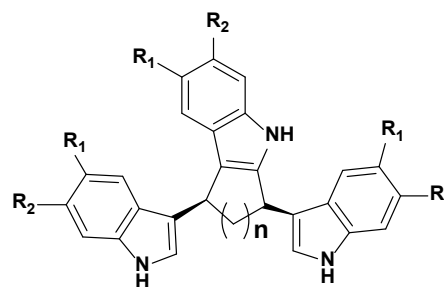
to predict the attributes of a particular chemical. A new compound may possess the same molecular function as that of the compound used in the development of a QSAR model, which would likely have the same activities and properties. Several types of QSAR models have been published in the last several years, which highlights the wide range of biological and physiological properties of these models. QSAR models have great potential for modeling and discovery of new compounds with different properties [19].

MATERIALS AND METHODS

1. Dataset

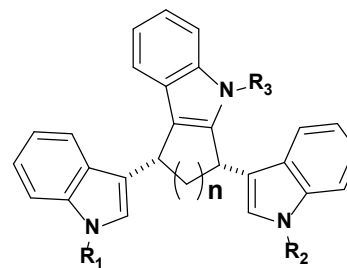
A set of 14 compounds of substituted indole derivatives was

Table 2. Chemical structure of substituted indole derivatives



Compound no.	N	R ₁	R ₂
7	3	H	H
8	3	Cl	H
9	3	H	Cl
10	4	H	H

Table 3. Chemical structure of substituted indole derivatives



Compound no.	N	R ₁	R ₂	R ₃
11	2	Ac	Ac	H
12	2	Ac	Ac	Ac
13	3	Ac	H	H
14	3	Ac	Ac	H

selected from the work of El-Sayed et al. (2016) [20] and is shown in Tables 1-3.

2. Descriptor generation

The construction of a numerical description of the molecular structure is the next phase in the model development process. ChemDraw was used to draw the structures of substituted indole derivatives, which were then optimized for energy. By using the software TSAR 3.3 for Windows, the energy-minimized structures were utilized to generate molecular descriptors of geometric, hydrophobic, topological, and electronic features (Table 4). The values of the descriptors selected for the multiple linear regression (MLR) model are presented in Table 5.

3. Pearson correlation analysis

We utilized Pearson's correlation matrix as a qualitative model (Table 5) to choose the appropriate descriptors for MLR analysis because each chemical had a high number of descrip-

tors. This method was used to select an appropriate collection of generated descriptors for MLR model calculations. The best MLR model was utilized to create a calibration model that could predict the antibacterial activity of the substituted indole derivative.

4. Multiple linear regressions

To create a QSAR model to estimate the antimicrobial activities of the substituted indole compounds selected in this study, we used MLR approaches. In QSARs, MLR is an efficient approach to solving regression difficulties. MLR determines that the predictor variables, commonly referred to as X, are mathematically independent (orthogonal). The rank of X is K, which denotes mathematical independence (the number of X variables). The awareness of associated descriptors is a shortcoming of MLR. The compound-to-variable ratio must be at least 5. Nevertheless, if the major challenge of variable selection is addressed and properly handled, MLR can be successfully employed in QSAR research.

Table 4. QSAR descriptors used in the study

S. No.	QSAR descriptor	Type
1	log P	Lipophilic
2	Zero order molecular connectivity index (${}^0\chi$)	Topological
3	First order molecular connectivity index (${}^1\chi$)	Topological
4	Second order molecular connectivity index (${}^2\chi$)	Topological
5	Valence zero order molecular connectivity index (${}^0\chi^v$)	Topological
6	Valence first order molecular connectivity index (${}^1\chi^v$)	Topological
7	Valence second order molecular connectivity index (${}^2\chi^v$)	Topological
8	Kier's alpha first order shape index ($\kappa\alpha_1$)	Topological
9	Kier's alpha second order shape index ($\kappa\alpha_2$)	Topological
10	Kier's first order shape index (κ_1)	Topological
11	Randic topological index	Topological
12	Balaban topological index	Topological
13	Wiener's topological index	Topological
14	Kier's second order shape index (κ_2)	Topological
15	Ionization potential	Electronic
16	Dipole moment (μ)	Electronic
17	Energy of highest occupied molecular orbital (HOMO)	Electronic
18	Energy of lowest unoccupied molecular orbital (LUMO)	Electronic
19	Total energy (Te)	Electronic
20	Nuclear energy (Nu. E)	Electronic
21	Molar refractivity (MR)	Steric

Table 5. Values of selected parameters used in regression analysis

Comp.	log P	χ^1_v	χ^2_v	κ_1	κ_2	R	J	W	EE	LUMO	HOMO	μ
1	4.98	10.61	8.42	19.47	7.80	14.88	1.00	2,185.00	-37,067.60	0.15	-8.03	2.71
2	5.19	11.15	9.02	20.38	8.05	15.31	1.03	2,323.00	-39,897.90	0.07	-8.17	3.93
3	5.25	11.61	9.56	20.38	8.05	15.31	1.03	2,323.00	-39,646.10	0.05	-8.14	4.16
4	5.38	11.11	8.76	20.38	8.34	15.38	1.04	2,420.00	-39,708.20	0.13	-8.01	3.29
5	6.93	12.63	10.61	23.14	9.08	16.56	1.04	3,114.00	-46,867.80	-0.20	-8.31	5.65
6	6.93	12.63	10.61	23.14	9.08	16.56	1.03	3,174.00	-46,522.30	-0.25	-8.27	3.33
7	5.77	11.61	9.11	21.30	8.90	15.88	1.07	2,580.00	-42,372.10	0.05	-7.91	2.39
8	7.33	13.13	10.96	24.07	9.63	17.06	1.06	3,360.00	-49,419.30	-0.32	-8.18	3.63
9	7.33	13.13	10.96	24.07	9.63	17.06	1.06	3,360.00	-49,420.60	-0.32	-8.18	3.63
10	6.17	12.11	9.47	22.22	9.47	16.38	1.09	2,769.00	-45,718.70	0.05	-7.91	2.00
11	5.37	12.85	10.16	25.93	10.44	18.02	1.06	3,881.00	-54,293.40	-0.36	-8.35	2.43
12	5.37	13.72	10.83	28.75	11.49	19.36	1.12	4,586.00	-63,219.40	-0.48	-8.59	2.62
13	5.77	12.48	9.81	24.07	9.95	17.20	1.07	3,275.00	-49,355.30	-0.09	-7.96	2.47
14	5.77	13.35	10.52	26.87	11.01	18.52	1.09	4,087.00	-56,391.20	-0.40	-8.09	1.89

5. Cross-validation

The 'leave one out' (LOO) technique was utilized for the cross-validation step of the models, where a model is built with N-1 chemicals, and the functionality of the nth molecule is calculated. Each molecule is left out of the model generation in turn, and its activity is calculated from the produced model. The predictive q² or cross-validated technique provides a validation of the model's accuracy as follows (Equation 2):

$$q^2 = (SD - PRESS / SD) \quad \text{Equation 2}$$

where SD is the total of square deviations from the mean of each activity and PRESS (predictive sum-of-squares) is the sum of the squared difference between actual and predicted values when the fitting method does not involve the compound. A high q² value is considered to reflect high predictability.

6. Molecular modeling

On Mac workstations, the docking interactions were calculated using Maestro 12.7 (Schrodinger 2021). The aim of this study was to determine how different ligands interact with the active site of the target receptor.

1) Selection and preparation of ligands

Ligand preparation was performed using the Ligprep wizard

of Maestro 12.7 (Schrodinger 2021). In this step, ligand structures were converted from a 2D to a 3D form, hydrogen atoms were added, discrepancies between bond lengths and angles were resolved, low-power structure and ring conformation were subjected to minimization, and OPLS 2005 force field was conducted. the remaining factors such as the ionization state were unaltered, and the specified chirality was retained [21, 22].

2) Preparation of the protein molecules

The protein's X-ray crystallographic composition (PDB ID: 2OLV and 5M18) was obtained from the Protein Data Bank (RSCB) and created using the protein preparation wizard of Maestro 12.7. Preprocessing, refinement, and minimization were the main components of the protein preparation wizard. Hydrogen atoms were added, zero-order bonds were created for metal, charges were fixed, missing disulfide bonds were rectified, bond orders were assigned, and side chains that were not close to the binding cavity were neutralized. Other problems such as overlapping, alternate position, or missing atoms were solved by adding hydrogen atoms, reorienting hydroxyl groups, water molecules, and amino acids. The selected protein was then reviewed and modified. Finally, the structure was refined using restrained minimization [23].

3) Receptor grid generation

Ligands bound within the X-ray crystal structure of the protein were utilized by Glide molecular docking for the iden-

tification of the active site receptor grid. As a result, grid-based molecular docking facilitated the binding of ligands in multiple potential conformations. The scaling factor was 0.25 Å and the partial charge cutoff of the Van der Waals radius was 1.0 Å. Sites, limitations, rotatable groups, and excluded volumes were also implemented [24].

4) Glide molecular docking

Docking was carried out using Extra Precision (XP) after ligand preparation, protein preparation, and grid generation on the active site of the target protein. Binding interactions and ligand flexibility were evaluated using Glide molecular docking, a system improvement for quick and accurate molecular docking. The binding energy, including ligand-protein interaction energies, was calculated in kcal/mol. H-bonding, lipophilic interactions, π - π stacking interactions, internal energy, Root Mean Square Deviation (RMSD), and desolvation energy were determined. The precise ligand-protein interactions were examined using the XP Visualizer. All selective ligands with an X-ray crystal structure, including the reference compound, were docked using Glide [25-27].

5) Docking evaluation

A docking score was obtained, and the conformation of the ligand-protein interaction was used to evaluate the corresponding docking. The compounds with the highest docking score and a strong interaction profile were the most active toward the target receptor.

RESULTS AND DISCUSSION

The structures of indole analogs (1-14) were first pre-optimized utilizing Hyperchem 6.03 and Molecular Mechanics Force Field (MM+), and the generated geometries were refined further using the semi-empirical Parametric Method-3 (PM3). For geometry optimization, we chose a normal gradient limit of 0.04 kJ/Å. Physicochemical characteristics were calculated with the TSAR 3.3 software for Windows using the lowest energy structure for each molecule. In addition, regression analysis was performed using the SPSS software package.

QSAR experiments were conducted utilizing Hansch and Fujita's linear free energy relationship (LFER) model to determine the substituent effect on antibacterial activity [28]. The standard antibiotics sultamicillin and ampicillin were not used in the model development because their structures differed

from those of the created compounds. The MIC values for biological activity were first translated into pMIC values (i.e., $-\log$ MIC, Table 6) and then used as dependent variables in the QSAR analysis. The molecular descriptors log of octanol-water partition coefficient ($\log P$), molar refractivity (MR), Kier's molecular connectivity (${}^0\chi, {}^0\chi_v, {}^1\chi, {}^1\chi_v, {}^2\chi, {}^2\chi_v$) and shape ($\kappa_1, \kappa\alpha_1, \kappa\alpha_2, \kappa\alpha_3$), the topological indices Randic topological index (R), Balaban topological index (J), and Wiener topological index (W), and total energy (Te), energies of highest occupied molecular orbital (HOMO) and lowest unoccupied molecular orbital (LUMO), dipole moment (μ), and electronic energy (Ele. E) [29-31] were used for model development and are summarized in Table 4. The values of the selected molecular descriptors used for model development are shown in Table 5.

The goal of this study was to create three distinct types of QSAR models to represent the antibacterial activity of the described compounds against *S. aureus*, MRSA standard, and MRSA isolates, viz. the mt-QSAR model. Compounds 1, 7, 10, and 11 were recognized as outliers in the regression analysis experiments and were not included in the dataset for QSAR model construction. Three categories of outliers are commonly defined in multivariate statistics [32]:

1. X/Y relationship outliers are compounds whose descrip-

Table 6. Antibacterial activity of indole derivatives (pMIC in $\mu\text{M}/\text{mL}$)

Compound no.	<i>S. aureus</i>	MRSA standard	MRSA isolate
1	0.89	1.49	1.49
2	2.13	2.13	1.83
3	2.17	2.17	1.87
4	2.11	2.11	1.81
5	2.21	1.91	1.61
6	1.61	1.61	1.61
7	2.12	1.82	1.52
8	2.22	1.92	1.92
9	2.22	1.92	1.62
10	2.14	1.84	1.54
11	0.69	0.69	0.69
12	1.02	1.02	1.02
13	1.26	1.56	1.56
14	0.70	1.00	1.00
Standard deviation	0.63	0.46	0.36
Sultamicillin	2.88	1.37	1.37
Ampicillin	2.35	0.84	0.84

Table 7. Correlation matrix for the antibacterial activity of indole derivatives

	<i>S. aureus</i>	MRSA std	MRSA isolate	log P	${}^2\chi^v$	κ_2	R	EE	μ
<i>S. aureus</i>	1.000								
MRSA Std	0.944	1.000							
MRSA isolate	0.889	0.950	1.000						
log P	0.321	0.090	0.182	1.000					
${}^2\chi^v$	-0.233	-0.503	-0.426	0.726	1.000				
κ_2	-0.795	-0.927	-0.874	0.101	0.664	1.000			
R	-0.773	-0.924	-0.876	0.122	0.704	0.995	1.000		
EE	0.741	0.907	0.864	-0.123	-0.714	-0.985	-0.997	1.000	
μ	0.802	0.693	0.587	0.320	-0.038	-0.619	-0.565	0.525	1.000

tors (X variables) and response variables (Y variables) have a different connection than the rest of the training dataset.

2. X outliers are compounds whose chemical descriptors do not fall inside the (remaining) training measurement range.

3. Only test or training samples are provided for Y outliers. They are chemicals for which the response reference value is incorrect.

As the activity and molecular descriptor range (Table 5) of these outliers were similar when compared to those of the other indole derivatives, they belonged to the category of Y outliers (substances for which the reference value of response is invalid) [32].

A correlation matrix (Table 7) was constructed to determine the relationship between the antibacterial activity of the reported compounds and their molecular descriptors. A high interrelationship was observed between the topological parameters Randic index (R) and Kier's second-order shape index (κ_2) ($r = 0.995$), and a low interrelationship was observed between the topological parameter valence second-order molecular connectivity index (${}^2\chi^v$) and the electronic parameter dipole moment (μ) ($r = -0.038$). The correlation between the antibacterial activity of indole derivatives against different bacterial strains and different molecular descriptors is shown in Table 8.

From the correlation matrix (Table 7), it was observed that the electronic parameter dipole moment (μ) dominated the description of the antibacterial activity of the reported compounds against *S. aureus* (Eq. 1).

1. LR-QSAR model for antibacterial activity against *S. aureus*

$$\text{pMICsa} = 0.445\mu + 0.227 \quad (1)$$

$$n = 10, r = 0.802, q^2 = 0.460, s = 0.366, F = 14.40$$

Table 8. Correlation of molecular descriptors with antibacterial activity of indole derivatives

	<i>S. aureus</i>	MRSA standard	MRSA isolate
log P	0.321	0.090	0.182
${}^1\chi^v$	-0.529	-0.754	-0.679
${}^2\chi^v$	-0.233	-0.503	-0.426
κ_1	-0.753	-0.916	-0.868
κ_2	-0.795	-0.927	-0.874
R	-0.773	-0.924	-0.876
EE	0.741	0.907	0.864
μ	0.802	0.693	0.587

where n is the number of data points, r is the correlation coefficient, q^2 is the cross-validated value, s is the standard error of the estimate, and F is the Fischer statistics.

To improve the correlation coefficient (r), the electronic parameter dipole moment (μ) was coupled with electronic energy, and r increased from 0.802 to 0.886 (Eq. 2).

2. MLR-QSAR model for antibacterial activity against *S. aureus*

$$\text{pMICsa} = 0.0000337\text{EE} + 0.361\mu + 2.293 \quad (2)$$

$$n = 10, r = 0.886, q^2 = 0.711, s = 0.304, F = 12.74$$

The developed model was cross-validated using the LOO technique. The q^2 value was more than 0.5 (Eq. 2), which showed that the developed model was valid [33]. Furthermore, the observed and predicted antibacterial activities were similar (Table 9), and thus the QSAR model for antibacterial activity against *S. aureus* (Eq. 2) was valid.

Kier's second-order shape index (κ_2) was found to be the most dominating descriptor in explaining the antibacterial activ-

Table 9. Comparison of observed and predicted antibacterial activity obtained by developed QSAR models

Comp.	<i>S. aureus</i>			MRSA Std			MRSA isolate		
	Obs.	Pre.	Res.	Obs.	Pre.	Res.	Obs.	Pre.	Res.
1	0.89	1.90	-1.01	1.49	2.29	-0.80	1.49	1.85	-0.36
2	2.13	2.19	-0.06	2.13	2.21	-0.08	1.83	1.83	0.00
3	2.17	2.27	-0.10	2.17	2.21	-0.03	1.87	1.91	-0.03
4	2.11	1.99	0.12	2.11	2.11	0.00	1.81	1.77	0.04
5	2.21	2.50	-0.29	1.91	1.85	0.05	1.61	1.72	-0.11
6	1.61	1.78	-0.17	1.61	1.85	-0.25	1.61	1.72	-0.11
7	2.12	1.62	0.50	1.82	1.92	-0.09	1.52	1.68	-0.16
8	2.22	1.77	0.45	1.92	1.66	0.25	1.92	1.63	0.29
9	2.22	1.77	0.45	1.92	1.66	0.25	1.62	1.63	-0.01
10	2.14	1.39	0.75	1.84	1.72	0.12	1.54	1.59	-0.06
11	0.69	1.23	-0.54	0.69	1.39	-0.70	0.69	1.24	-0.56
12	1.02	0.99	0.03	1.02	1.03	-0.01	1.02	0.97	0.05
13	1.26	1.41	-0.15	1.56	1.56	0.01	1.56	1.42	0.14
14	0.70	0.99	-0.29	1.00	1.19	-0.19	1.00	1.16	-0.16

ity of the reported compounds against MRSA standard (Table 8).

3. LR-QSAR model for antibacterial activity against MRSA standard

$$\text{pMICMRSA Std} = -0.342\kappa_2 + 4.959 \quad (3)$$

$$n = 10, r = 0.927, q^2 = 0.803, s = 0.172, F = 48.61$$

It is evident from Eq. 3 that the antibacterial activity of the reported compounds against MRSA standard was negatively correlated to Kier's second-order shape index (κ_2), i.e., the antibacterial activity of these compounds decreased with the increase in their κ_2 value and vice versa, which was evidenced by the lowest antibacterial activity of compound 12 (1.02 $\mu\text{M}/\text{mL}$, Table 6) having the highest κ_2 value (11.49, Table 5). This illustrates the negative correlation. The kappa indices of molecular size and flexibility comprise a collection of very useful second-generation topological indices [29]. According to Kier, a molecule's shape can be divided into qualities, each of which is characterized by the number of bonds with different path lengths. The relationship between the number of paths of length l in the molecule i , IP_i , and some reference values predicated on molecules with a given number of atoms, n , in which the values of IP are maximal and minimal, IP_{max} and IP_{min} , provides the foundation for developing a relative index of form. The expression for the first-order shape property, κ_1 , is as follows:

$$\kappa_1 = n(n-1)2/(1Pi)2$$

The second- and third-order kappa indices are defined as follows:

$$\kappa_2 = (n-1)(n-2)/(2Pi)2$$

The antibacterial activity of the reported compounds against MRSA isolate was best explained by the topological parameter Randic index (R) (Table 8).

4. LR-QSAR model for antibacterial activity against MRSA isolate

$$\text{pMICMRSA isolate} = -0.213 R + 5.17 \quad (4)$$

$$n = 10, r = 0.876, q^2 = 0.667, s = 0.168, F = 26.33$$

Similar to MRSA standard, the antibacterial activity of the reported compounds against MRSA isolate of the synthesized compounds was also negatively correlated with R. The coupling of the topological parameter Randic index (R) with valence second-order molecular connectivity index (${}^2\chi^v$) resulted in the best model for explaining the antibacterial activity of the reported compounds against MRSA isolate (Eq. 5).

5. MLR-QSAR model for antibacterial activity against MRSA isolate

$$\text{pMICMRSA isolate} = 0.152 {}^2\chi^v - 0.278 R + 4.71 \quad (5)$$

$$n = 10, r = 0.916, q^2 = 0.702, s = 0.149, F = 18.31$$

The high q^2 value ($q^2 > 0.5$) obtained using the LOO

technique, as well as the low residual activity values from Eq. 5, demonstrated the validity and predictability of the QSAR model for antibacterial activity against MRSA isolate (Table 9). In summary, the QSAR findings showed that topological parameters such as valence second-order molecular connectivity index (${}^2\chi^v$), Randic index (R), and Kier's second-order shape index (κ_2), as well as electronic parameters such as electronic energy (EE) and dipole moment (μ), are important for describing the antibacterial activity of the disclosed indole derivatives. Additionally, the significant residual value of outliers justified their removal before model construction. The range of antibacterial activities of the synthesized compounds in this study was within one order of magnitude, whereas the biological activities of compounds should normally span 2-3 orders of magnitude for QSAR analyses. This is consistent with the results of Narasimhan et al. [34], who found that the QSAR model's accuracy is based on its predictive capacity even when the activity data are limited. The presence of a minimal standard deviation of bioactivity confirms its application in QSAR research when biological activity data are restricted [34, 35]. The minimum standard deviation observed in the antimicrobial activity data justified its use in QSAR studies.

6. Molecular docking studies

To evaluate the antibacterial activity of the reported compounds, we selected two proteins (penicillin-binding protein, source: *S. aureus* PDB 2OLV; and penicillin-binding protein 2a, source: MRSA PDB 5M18) from the Protein Data Bank (rcsb.org) and subjected them to molecular docking studies [35]. Sultamicillin and ampicillin were selected as standards. For *S. aureus*, compound 12 showed a better binding score (-6.247 kcal/mol) by π - π interactions with Lys155, hydrophobic interactions with Phe158, Leu159, Ile195, Tyr196, Pro231, Val232, and Pro233, and polar interactions with Ser147, Gln152, Ser160, and Gln161 with reference to sultamicillin (by interacting with Lys155 and Tyr196) and ampicillin (by interacting with Ash156 and Pro231). For MRSA, compound 2 showed a better docking score (-5.832 kcal/mol) by π - π interactions with Lys148 and Asp275, hydrophobic interactions with Phe158, Leu159, Tyr191, Ile195, Tyr196, Pro231, and Pro233, and polar interactions with Gln152, Ser160, Gln161, Thr202, and Gln 232 in comparison to sultamicillin (by interacting with Met372) and ampicillin (by interacting with Lys155 and Pro231). Docking scores and the main binding interactions of the compounds are

shown in Table 10. A 2D interaction diagram of compounds 12 and 2 is shown in Fig. 1.

CONCLUSION

In describing the antibacterial activities of the reported indole derivatives, QSAR analysis revealed the importance of topological parameters such as valence second-order molecular connectivity index (${}^2\chi^v$), Randic index (R), and Kier's second-order shape index (κ_2), as well as electronic parameters such as electronic energy (EE) and dipole moment (μ). Compounds with high electronic energy and dipole moment seemed to be effective antibacterial agents against *S. aureus*, indole derivatives with lower q_2 values seemed to be effective antibacterial agents against an MRSA standard strain, and compounds with a low R-value and a high ${}^2\chi^v$ value seemed to be effective antibacterial agents against MRSA isolate. We also performed molecular docking studies of all selected compounds and found that compounds 12 and 2 showed better binding scores against penicillin-binding protein and penicillin-binding protein 2a, respectively.

Table 10. Docking score of selected compounds against PDB: 2OLV and 5M18

S. No.	Compound no.	Docking score (Kcal/mol) (PDB: 2OLV)	Docking score (Kcal/mol) (PDB:5M18)
1	1	-5.136	-4.715
2	2	-5.160	-5.832
3	3	-5.06	-4.755
4	4	-4.812	-5.413
5	5	-4.707	-5.366
6	6	-4.692	-5.143
7	7	-4.620	-5.076
8	8	-4.893	-4.926
9	9	-4.463	-2.189
10	10	-4.174	-4.396
11	11	-5.358	-4.026
12	12	-6.247	-4.550
13	13	-4.370	-5.412
14	14	-4.066	-5.486
15	Sultamicillin	-5.280	-5.519
16	Ampicillin	-5.358	-4.926

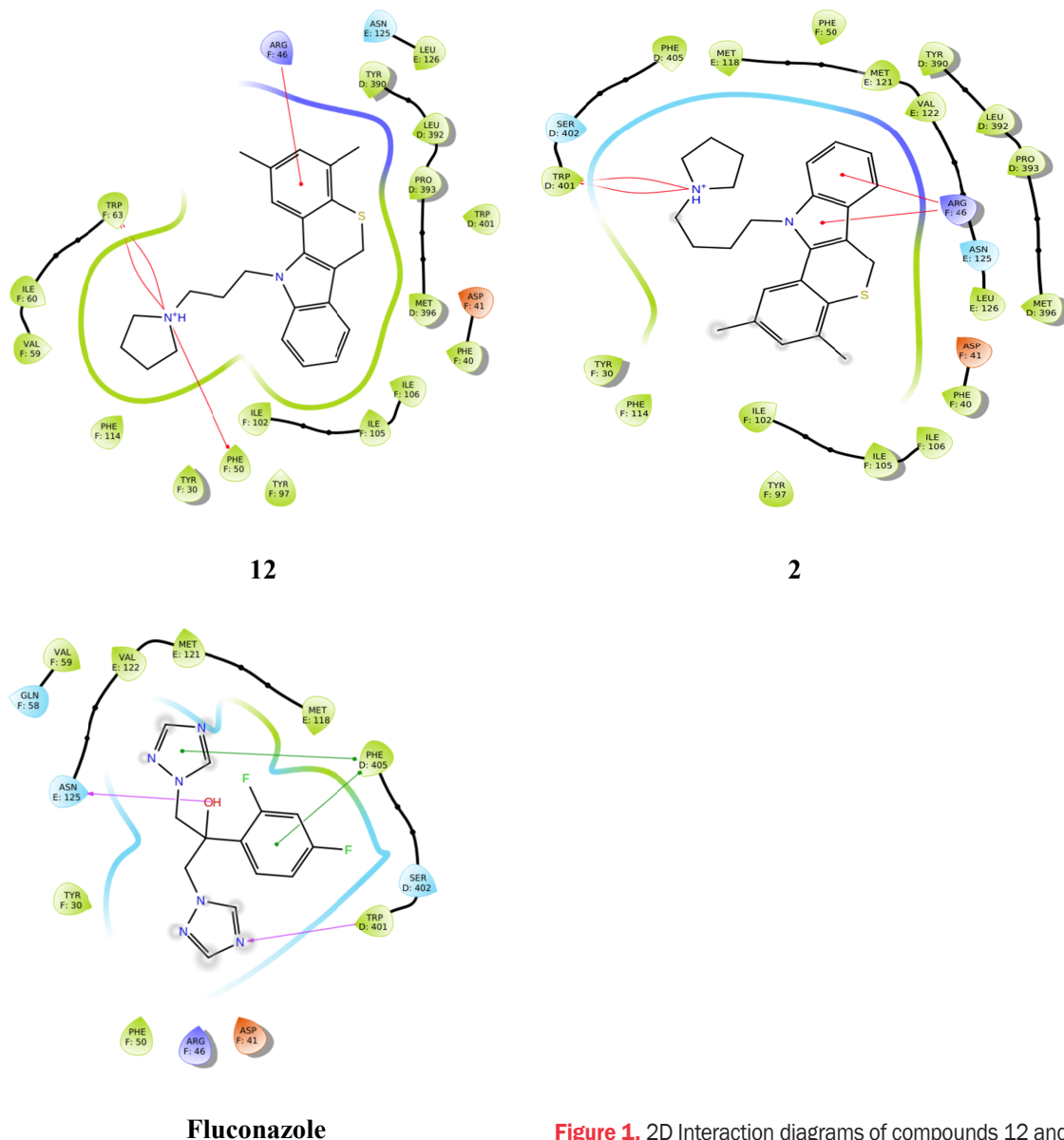


Figure 1. 2D Interaction diagrams of compounds 12 and 2.

ACKNOWLEDGEMENTS

Authors are thankful to Central University of Punjab, Bathinda and DST-FIST for providing infrastructural support.

CONFLICTS OF INTEREST

The authors declare no conflict of interest.

FUNDING

This research did not receive any specific grant from funding

agencies in the public, commercial, or not-for-profit sectors.

ORCID

Mridul Shah, <https://orcid.org/0009-0001-1264-9451>

Adarsh Kumar, <https://orcid.org/0000-0001-8035-5984>

Ankit Kumar Singh, <https://orcid.org/0000-0001-6129-0169>

Harshwardhan Singh, <https://orcid.org/0000-0002-2667-173X>

Balasubramanian Narasimhan,

<https://orcid.org/0000-0002-9627-094X>

REFERENCES

- Kumavath R. Antibacterial agents. London: IntechOpen; 2017.
- Harbarth S, Balkhy HH, Goossens H, Jarlier V, Kluytmans J, Laxminarayan R, et al. Antimicrobial resistance: one world, one fight! *Antimicrob Resist Infect Control*. 2015;4:49.
- Gupta PD, Birdi TJ. Development of botanicals to combat antibiotic resistance. *J Ayurveda Integr Med*. 2017;8(4):266-75.
- Cohen ML. Epidemiology of drug resistance: implications for a post-antimicrobial era. *Science*. 1992;257(5073):1050-5.
- Raju PAG, Mallikarjunarao R, Gopal KV, Sreeramulu J, Krishnamurthi KP, Reddy SR. Synthesis and biological activity of some new indole derivatives containing pyrazole moiety. *J Chem Pharm Res*. 2013;5(10):21-7.
- Walmik P, Saundane AR. Synthesis of novel indolyl-azetidinone and thiazolidinone derivatives as a potent antioxidant, antimicrobial and antitubercular agents. *Der Pharma Chem*. 2014;6(4):70-9.
- Guerra AS, Malta DJ, Laranjeira LP, Maia MB, Colaço NC, de Lima Mdo C, et al. Anti-inflammatory and antinociceptive activities of indole-imidazolidine derivatives. *Int Immunopharmacol*. 2011;11(11):1816-22.
- Iddalingamurthy E, Mahadevan KM, Jagadeesh NM, Kumara MN. Synthesis and docking study of 3-(N-alkyl/aryl piperidyl) indoles with serotonin-5HT₁ and CCR2 antagonist receptors. *Int J Pharm Pharma Sci*. 2014;6(4):475-82.
- Muralikrishna S, Raveendrareddy P, Ravindranath LK, Hari-krishna S, Jagadeeswara Rao P. Synthesis Characterization and antitumor activity of thiazole derivatives containing indole moiety bearing-tetrazole. *Der Pharma Chem*. 2013;5(6):87-93.
- Raju GN, Sai KB, Prasanna ML, Aparna V, Chandana K, Nadendla RR. Synthesis, characterization and biological activity of some 1, 3, 4-oxadiazole derivatives with indole moiety. *Der Pharm Lett*. 2015;7(5):153-9.
- Estevão MS, Carvalho LC, Ribeiro D, Couto D, Freitas M, Gomes A, et al. Antioxidant activity of unexplored indole derivatives: synthesis and screening. *Eur J Med Chem*. 2010;45(11):4869-78.
- Rohini RM, Manjunath M. Synthesis and anti-convulsant activity of triazothiole/thiazolyl thiazolidinone derivatives of indole. *Der Pharma Chem*. 2012;4(6):2438-41.
- Delorenzi JC, Attias M, Gattass CR, Andrade M, Rezende C, da Cunha Pinto Â, et al. Antileishmanial activity of an indole alkaloid from *Peschiera australis*. *Antimicrob Agents Chemother*. 2001;45(5):1349-54.
- Mondal P, Jana S, Balaji A, Ramakrishna R, Kanthal L. Synthesis of some new isoxazoline derivatives of chalconised indoline 2-one as a potential analgesic, antibacterial and anthelmintic agents. *J Young Pharm*. 2012;4(1):38-41.
- Poojitha J, Mounika KN, Raju GN, Nadendla RR. Indole: the molecule of diverse pharmacological activities. *World J Pharm Res*. 2015;4(12):656-66.
- Rose WC. The nutritive significance of the amino acids. *Physiol Rev*. 1938;18(1):109-36.
- Dhani R, Avinash A, Salenaagina SK, Saicharan Teja MV, Masthanaiah P, Rathnam R, et al. Indole: the molecule of diverse pharmacological activities. *J Chem Pharm Res*. 2011;3(5):519-23.
- Rajandran T, Prabhu R, Prabhu M. Molecular docking studies of indole derivatives containing cyanide group as hepatitis C N5b polymerase inhibitor. *Pharma Innov*. 2015;4(9):43-8.
- Nantasenamat C, Isarankura-Na-Ayudhya C, Naenna T, Prachayasittikul V. A practical overview of quantitative structure-activity relationship. *EXCLI J*. 2009;8:74-88.
- El-Sayed MT, Suzen S, Altanlar N, Ohlsen K, Hilgeroth A. Discovery of bisindolyl-substituted cycloalkane-anellated indoles as novel class of antibacterial agents against *S. aureus* and MRSA. *Bioorg Med Chem Lett*. 2016;26(1):218-21.
- Van Den Driessche G, Fourches D. Adverse drug reactions triggered by the common HLA-B*57:01 variant: a molecular docking study. *J Cheminform*. 2017;9:13.
- Sastry GM, Adzhigirey M, Day T, Annabhimoju R, Sherman W. Protein and ligand preparation: parameters, protocols, and influence on virtual screening enrichments. *J Comput Aided Mol Des*. 2013;27(3):221-34.
- Kumar S, Singh J, Narasimhan B, Shah SAA, Lim SM, Ramasamy K, et al. Reverse pharmacophore mapping and molecular docking studies for discovery of GTPase HRas as promising drug target for bis-pyrimidine derivatives. *Chem Cent J*. 2018;12(1):106.
- Sharma V, Sharma PC, Kumar V. In silico molecular docking analysis of natural pyridoacridines as anticancer agents. *Adv Chem*. 2016;2016:5409387.
- Singh J, Kumar M, Mansuri R, Sahoo GC, Deep A. Inhibitor designing, virtual screening, and docking studies for methyltransferase: a potential target against dengue virus. *J Pharm Bioallied Sci*. 2016;8(3):188-94.
- Friesner RA, Murphy RB, Repasky MP, Frye LL, Greenwood JR, Halgren TA, et al. Extra precision glide: docking and scoring incorporating a model of hydrophobic enclosure for protein-ligand complexes. *J Med Chem*. 2006;49(21):6177-96.
- Lenselink EB, Louvel J, Forti AF, van Veldhoven JPD, de Vries H, Mulder-Krieger T, et al. Predicting binding affinities for GPCR ligands using free-energy perturbation. *ACS Omega*. 2016;1:293-304.
- Hansch C, Fujita T. ρ - σ - π Analysis. A method for the correlation

- of biological activity and chemical structure. *Am Chem Soc.* 1964;86(8):1616-26.
29. Kier LB, Hall LH. The kappa indices for modeling molecular shape and flexibility. In: Devillers J, Balaban AT, editors. *Topological indices and related descriptors in QSAR and QSPR*. London: CRC Press; 1999. p. 465-500.
30. Randic M. Characterization of molecular branching. *J Am Chem Soc.* 1975;97(23):6609-15.
31. Balaban AT. Highly discriminating distance-based topological index. *Chem Phys Lett.* 1982;89(5):399-404.
32. Furusjö E, Svenson A, Rahmberg M, Andersson M. The importance of outlier detection and training set selection for reliable environmental QSAR predictions. *Chemosphere.* 2006;63(1):99-108.
33. Golbraikh A, Tropsha A. Beware of q²! *J Mol Graph Model.* 2002;20(4):269-76.
34. Narasimhan B, Judge V, Narang R, Ohlan R, Ohlan S. Quantitative structure-activity relationship studies for prediction of antimicrobial activity of synthesized 2,4-hexadienoic acid derivatives. *Bioorg Med Chem Lett.* 2007;17(21):5836-45.
35. Kumar A, Singh AK, Thareja S, Kumar P. A review of pyridine and pyrimidine derivatives as anti-MRSA agents. *Antiinfect Agents.* 2023;21(2):e050722206610.